

New results on inclusive $B \rightarrow X_u \ell \nu$ decay from the Belle experiment

Lu Cao^{1,*}

*University of Bonn,
Nussallee 12, Bonn, Germany*

E-mail: cao@physik.uni-bonn.de

We report on the measurement of inclusive charmless semileptonic B decays $B \rightarrow X_u \ell \nu$. The analysis makes use of hadronic tagging and is performed on the full data set of the Belle experiment comprising 772 million $B\bar{B}$ pairs. In the proceedings, the preliminary results of measurements of partial branching fractions and the CKM matrix element $|V_{ub}|$ are presented.

*40th International Conference on High Energy physics - ICHEP2020
July 28 - August 6, 2020
Prague, Czech Republic (virtual meeting)*

¹On behalf of the Belle collaboration.

*Speaker

1. Introduction

In the Standard Model of particle physics (SM), the Cabibbo-Kobayashi-Maskawa (CKM) matrix [1, 2] describes the quark mixing and accounts for CP -violation in the quark sector. One of the crucial tests of the SM is precise determination of the magnitude of the matrix elements. In b -flavor scope, the corresponding world averages of $|V_{ub}|$ from both exclusive and inclusive determinations [3] are

$$\begin{aligned} |V_{ub}^{\text{excl.}}| &= (3.67 \pm 0.09 \pm 0.12) \times 10^{-3}, \\ |V_{ub}^{\text{incl.}}| &= \left(4.32 \pm 0.12^{+0.12}_{-0.13}\right) \times 10^{-3}, \end{aligned} \quad (1)$$

where the uncertainties are from experiment and theory. The disagreement between them is about three standard deviations.

On the other hand, the experimental measurement of the inclusive semileptonic decay $B \rightarrow X_u \ell \nu$ is challenging due to the large background from the CKM-favoured $B \rightarrow X_c \ell \nu$ decay. Fig. 1 illustrates the $B \rightarrow X_u \ell \nu$ and $B \rightarrow X_c \ell \nu$ decays with the generator-level distributions in two important kinematic variables: the invariant mass of hadronic system M_X and the lepton energy in the signal B rest frame E_ℓ^B . It's shown that the clear separation of the signal decay is only possible in certain kinematic regions, e.g. the endpoint of lepton energy or the low M_X region. The details of the reconstruction and separation strategy is described in Sec. 2. The preliminary results on the measured partial branching fractions and the $|V_{ub}|$ values are presented in Sec. 3.

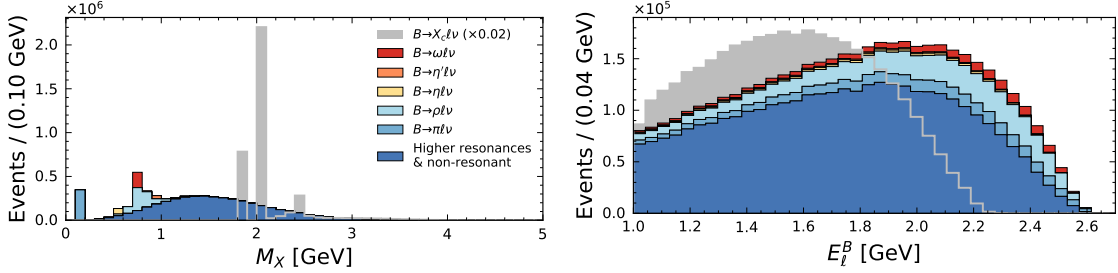


Figure 1: The generator-level M_X and E_ℓ^B distributions of the $B \rightarrow X_u \ell \nu$ decay comparing to that of $B \rightarrow X_c \ell \nu$ decay. The $B \rightarrow X_c \ell \nu$ component (gray) is scaled down by a factor of 50 for illustration.

2. Analysis strategy

The data used in this analysis were recorded with the Belle detector [4] at the KEKB accelerator complex [5] with a center-of-mass energy of $\sqrt{s} = 10.58$ GeV. The full data set contains an integrated luminosity of 711 fb^{-1} and corresponds to 772 million $\Upsilon(4S) \rightarrow B\bar{B}$ events. The Monte Carlo (MC) simulated events are generated by EVTGEN [6] and the detector response is modeled using GEANT3 [7]. The signal $B \rightarrow X_u \ell \nu$ MC sample is a combination of resonances and non-resonant decay using a hybrid modelling approach [8, 9]. The non-resonant component is based on the theory calculation of Ref. [10] with the model parameters in the Kagan-Neubert scheme from Ref. [11].

The hadronic decays of one of the B mesons are reconstructed via the full reconstruction algorithm [12] based on neural networks. In total, over 1104 decay cascades are considered and

reconstructed. The efficiencies for charged and neutral B mesons are 0.28% and 0.18%, respectively [13]. The output classifier score of this algorithm presents the quality of the reconstructed candidates. We select the best candidate of B_{tag} for each event. In addition, we require the beam-constrained mass $M_{\text{bc}} = \sqrt{(\sqrt{s}/2)^2 - |\mathbf{p}_{\text{tag}}|^2} > 5.27$ GeV to suppress continuum processes ($e^+e^- \rightarrow q\bar{q}$, $q = u, d, s, c$) and beam background.

All tracks and clusters not used in the construction of the B_{tag} candidate are used to reconstruct the signal side. With the fully reconstructed four-momentum of B_{tag} and the known beam-momentum, the signal B rest frame can be defined as

$$p_{\text{sig}} = p_{e^+e^-} - \left(\sqrt{m_B^2 + |\mathbf{p}_{\text{tag}}|^2}, \mathbf{p}_{\text{tag}} \right). \quad (2)$$

The signal lepton with $E_\ell^B = |\mathbf{p}_\ell^B| > 1$ GeV is used to identify the semileptonic decays. Here the small correction of the lepton mass term to the energy of the lepton is neglected. A veto on lepton-pair mass is applied to reject the lepton from J/ψ decay and photon conversions. In addition, the charge of lepton is required to be opposite to B_{tag} for the charged B case. With the signal lepton selected, the four-momentum of hadronic system p_X is defined as a sum of the four-momenta of tracks and clusters which are not involved in reconstructing the B_{tag} and signal lepton. Furthermore, we reconstruct the missing mass squared and the four-momentum transfer squared q^2 as

$$MM^2 = (p_{\text{sig}} - p_X - p_\ell)^2, \quad q^2 = (p_{\text{sig}} - p_X)^2. \quad (3)$$

We utilise a machine learning based classification with boosted decision trees (BDTs) to separate the signal $B \rightarrow X_u \ell \nu$ decay from the background events which are dominated by $B \rightarrow X_c \ell \nu$. The feature variables used for training include MM^2 , the number of charged kaons and K_s^0 , the total charge of event, the vertex fit χ^2/dof between the hadronic system and signal lepton, and the MM^2 and angular information of a partially reconstructed $B \rightarrow D^* \ell \nu, D^* \rightarrow D \pi_{\text{slow}}$ decay with the slow pions candidates, where $p_{\pi_{\text{slow}}}^{\text{cms}} < 0.22$ GeV. Due to the small difference between the masses of D and D^* , the flight directions of the π_{slow} and D^* are strongly correlated and we estimate the energy of D^* as $E_{D^*} \approx m_{D^*} \times E_{\pi_{\text{slow}}} / (m_{D^*} - m_D)$. On the BDT classifier output, we choose a selection criteria that reject 98.1% of $B \rightarrow X_c \ell \nu$ decays and retain 24.8% of $B \rightarrow X_u \ell \nu$ signal decays. The selection efficiency on data is 2.3%.

In addition, the B_{tag} reconstruction efficiency is calibrated using a data-driven approach described in Ref. [14]. The uncertainty of calibration is considered in systematics. We also apply a continuum efficiency correction to the simulated sample by comparing the difference to the number of reconstructed off-resonance events in data.

3. Partial branching fractions and $|V_{ub}|$ results

A binned likelihood fit is performed to extract the signal yield, where the systematic uncertainties are incorporated via nuisance-parameter constraints. The fit uses MC templates for background, and for signal in and out-side of the selected phase-space regions. In total, we carry out five separate fits to measure the three partial branching fractions as summarised in Table 1. Fig. 2 shows the main fit results. The result based on the two-dimensional fit of M_X and q^2 , i.e.

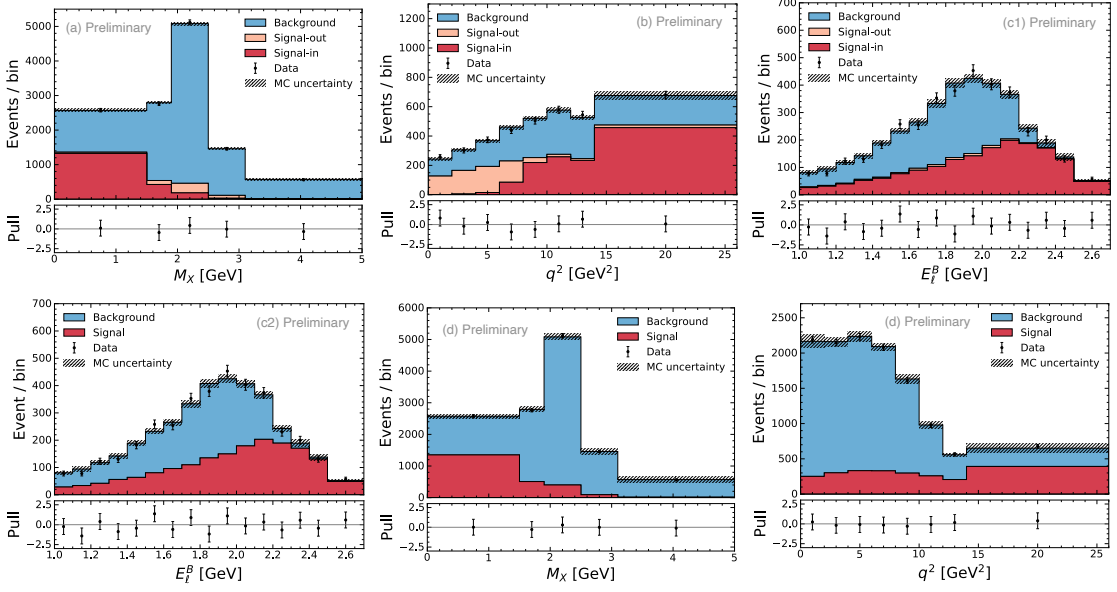


Figure 2: The post-fit distributions for various phase-space regions and kinematic variables. The distributions of the two-dimensional fit (d) are shown on the projections of M_X and q^2 .

$\Delta\text{BF} = (1.56 \pm 0.06 \pm 0.12) \times 10^{-3}$, is in a good agreement with the one obtained by fitting the lepton spectrum, covering the same phase-space region. It also agrees well with the most precise measurement to date of this region [15], where $\Delta\text{BF} = (1.55 \pm 0.12) \times 10^{-3}$. For other phase-space regions, the measured partial branching fractions are also compatible with the previous measurements [16].

Based on the measured partial branching fractions, we calculate the $|V_{ub}|$ value with the theoretical input of decay rate as

$$|V_{ub}| = \sqrt{\frac{\Delta\mathcal{B}(B \rightarrow X_u \ell \nu)}{\tau_B \Delta\Gamma(B \rightarrow X_u \ell \nu)}}, \quad (4)$$

where the average B meson lifetime is taken as (1.579 ± 0.004) ps [17] and the state-of-the-art theory predictions on $\Delta\Gamma$ are listed in Table 2. Table 3 summarises the measured $|V_{ub}|$ values. To quote a single value for $|V_{ub}|$ we adapt the procedure of Ref. [17] and calculate a simple arithmetic

Fit	Fit variable	Phase-space region	$10^3 \Delta\text{BF}$
(a)	M_X	$E_\ell^B > 1 \text{ GeV}, M_X < 1.7 \text{ GeV}$	$1.04 \pm 0.04 \pm 0.07$
(b)	q^2	$E_\ell^B > 1 \text{ GeV}, M_X < 1.7 \text{ GeV}, q^2 > 8 \text{ GeV}^2$	$0.70 \pm 0.06 \pm 0.09$
(c1)	E_ℓ^B	$E_\ell^B > 1 \text{ GeV}, M_X < 1.7 \text{ GeV}$	$1.09 \pm 0.05 \pm 0.10$
(c2)	E_ℓ^B	$E_\ell^B > 1 \text{ GeV}$	$1.66 \pm 0.08 \pm 0.17$
(d)	$M_X - q^2$	$E_\ell^B > 1 \text{ GeV}$	$1.56 \pm 0.06 \pm 0.12$

Table 1: The measured partial branching fractions for various phase-space regions. The first uncertainty is statistical and the second one is systematics.

Phase-space region	BLNP [20]	DGE [21, 22]	GGOU [23]	ADFR [24, 25]
$M_X < 1.7\text{GeV}$	$45.2^{+5.4}_{-4.6}$	$42.3^{+5.8}_{-3.8}$	$43.7^{+3.9}_{-3.2}$	$52.3^{+5.4}_{-4.7}$
$M_X < 1.7\text{GeV}, q^2 > 8\text{GeV}^2$	$23.4^{+3.4}_{-2.6}$	$24.3^{+2.6}_{-1.9}$	$23.3^{+3.2}_{-2.4}$	$31.1^{+3.0}_{-2.6}$
$E_\ell^B > 1\text{GeV}$	$61.5^{+6.4}_{-5.1}$	$58.2^{+3.6}_{-3.0}$	$58.5^{+2.7}_{-2.3}$	$61.5^{+5.8}_{-5.1}$

Table 2: The theory predicted decay rates in the three phase-space regions (ps^{-1}).

Fit	$10^3 V_{ub} ^{\text{BLNP}}$	$10^3 V_{ub} ^{\text{DGE}}$	$10^3 V_{ub} ^{\text{GGOU}}$	$10^3 V_{ub} ^{\text{ADFR}}$
(a)	$3.81^{+0.08,+0.13,+0.21}_{-0.08,-0.13,-0.21}$	$3.99^{+0.08,+0.14,+0.20}_{-0.08,-0.14,-0.26}$	$3.88^{+0.08,+0.13,+0.15}_{-0.08,-0.14,-0.16}$	$3.55^{+0.07,+0.12,+0.17}_{-0.07,-0.12,-0.17}$
(b)	$4.35^{+0.18,+0.26,+0.26}_{-0.18,-0.28,-0.28}$	$4.27^{+0.17,+0.26,+0.18}_{-0.18,-0.28,-0.21}$	$4.36^{+0.18,+0.27,+0.24}_{-0.18,-0.28,-0.27}$	$3.77^{+0.15,+0.23,+0.17}_{-0.16,-0.24,-0.17}$
(c1)	$3.90^{+0.09,+0.17,+0.21}_{-0.10,-0.18,-0.21}$	$4.08^{+0.10,+0.18,+0.20}_{-0.10,-0.19,-0.26}$	$3.97^{+0.09,+0.18,+0.15}_{-0.10,-0.19,-0.16}$	$3.63^{+0.09,+0.16,+0.17}_{-0.09,-0.17,-0.17}$
(c2)	$4.14^{+0.10,+0.20,+0.18}_{-0.10,-0.22,-0.20}$	$4.25^{+0.10,+0.21,+0.11}_{-0.10,-0.22,-0.12}$	$4.24^{+0.10,+0.21,+0.09}_{-0.10,-0.22,-0.10}$	$4.14^{+0.10,+0.20,+0.18}_{-0.10,-0.22,-0.18}$
(d)	$4.01^{+0.08,+0.15,+0.18}_{-0.08,-0.16,-0.19}$	$4.12^{+0.08,+0.16,+0.11}_{-0.09,-0.16,-0.12}$	$4.11^{+0.08,+0.16,+0.08}_{-0.09,-0.16,-0.09}$	$4.01^{+0.08,+0.15,+0.18}_{-0.08,-0.16,-0.18}$

Table 3: The extracted $|V_{ub}|$ values based on four theoretical inputs on the decay rates. The first uncertainty is statistical, the second one is systematic and the last term comes from the corresponding theory calculation.

average of the most precise determinations for the phase-space region $E_\ell^B > 1\text{ GeV}$, obtaining

$$|V_{ub}| = (4.06 \pm 0.09 \pm 0.16 \pm 0.15) \times 10^{-3}. \quad (5)$$

This value is smaller than the previous inclusive measurements of $|V_{ub}|$ in Ref. [16, 18]. The compatibility with the exclusive measurement of $|V_{ub}|$ in Eq.1 is 1.4 standard deviations; it is also compatible with the value expected from CKM unitarity from a global fit of Ref. [19] of $|V_{ub}| = (3.62^{+0.11}_{-0.08}) \times 10^{-3}$ within 1.6 standard deviations.

4. Summary and outlook

The preliminary results are obtained with the hadronic tagged analysis based on the full Belle data set. The measured partial branching fractions for the three phase-space regions are compatible with the previous measurements. The preliminary $|V_{ub}|$ value extracted in this analysis is larger but compatible with the exclusive determination within 1.4 standard deviations. Based on this preliminary result, the final analysis will incorporate a few modifications, including the aspects of increasing the simulated sample size and considering additional systematics accounting for the signal modeling. The separate-mode branching fractions for B^+/B^0 and e/μ will be also provided.

References

- [1] N. Cabibbo, *Phys. Rev. Lett.* **10**, 531 (1963).
- [2] M. Kobayashi and T. Maskawa, *Prog. Theor. Phys.* **49**, 652 (1973).

- [3] Y. S. Amhis *et al.* (HFLAV), (2019), [arXiv:1909.12524 \[hep-ex\]](#) .
- [4] A. Abashian *et al.*, *Nucl. Instrum. Meth.* **A479**, 117 (2002), also see detector section in J. Brodzicka *et al.*, *Prog. Theor. Exp. Phys.* **2012**, 04D001 (2012).
- [5] S. Kurokawa and E. Kikutani, *Nucl. Instr. and Meth.* **A499**, 1 (2003), and other papers included in this Volume; T. Abe *et al.*, *Prog. Theor. Exp. Phys.* **2013**, 03A001 (2013) and references therein.
- [6] D. J. Lange, *Nucl. Instr. and Meth.* **A462**, 152 (2001).
- [7] R. Brun, F. Bruyant, M. Maire, A. C. McPherson, and P. Zancarini, *CERN-DD-EE-84-1* (1987).
- [8] C. Ramirez, J. F. Donoghue, and G. Burdman, *Phys. Rev.* **D 41**, 1496 (1990).
- [9] M. Prim *et al.* (Belle Collaboration), *Phys. Rev. D* **101**, 032007 (2020).
- [10] F. De Fazio and M. Neubert, *JHEP* **06**, 017 (1999).
- [11] O. Buchmuller and H. Flacher, *Phys. Rev. D* **73**, 073008 (2006), [arXiv:hep-ph/0507253](#) .
- [12] M. Feindt, F. Keller, M. Kreps, T. Kuhr, S. Neubauer, D. Zander, and A. Zupanc, *Nucl. Instrum. Meth. A* **654**, 432 (2011).
- [13] A. Bevan *et al.*, *Eur. Phys. J. C* **74**, 3026 (2014, Page 95).
- [14] R. Glattauer *et al.* (Belle Collaboration), *Phys. Rev.* **D93**, 032006 (2016).
- [15] J. Lees *et al.* (BaBar Collaboration), *Phys. Rev. D* **95**, 072001 (2017).
- [16] J. Lees *et al.* (BaBar Collaboration), *Phys. Rev. D* **86**, 032004 (2012).
- [17] P. Zyla *et al.* (Particle Data Group), *Prog. Theor. Exp. Phys.* **2020 083C01** (2020).
- [18] P. Urquijo *et al.* (Belle Collaboration), *Phys. Rev. Lett.* **104**, 021801 (2010).
- [19] J. Charles, A. Hocker, H. Lacker, S. Laplace, F. Le Diberder, J. Malcles, J. Ocariz, M. Pivk, and L. Roos (CKMfitter Group), *Eur. Phys. J. C* **41**, 1 (2005).
- [20] B. O. Lange, M. Neubert, and G. Paz, *Phys. Rev. D* **72**, 073006 (2005).
- [21] J. R. Andersen and E. Gardi, *JHEP* **01**, 097 (2006).
- [22] E. Gardi, *Frascati Phys. Ser.* **47**, 381 (2008).
- [23] P. Gambino, P. Giordano, G. Ossola, and N. Uraltsev, *JHEP* **10**, 058 (2007).
- [24] U. Aglietti, F. Di Lodovico, G. Ferrera, and G. Ricciardi, *Eur. Phys. J. C* **59**, 831 (2009).
- [25] U. Aglietti, G. Ferrera, and G. Ricciardi, *Nucl. Phys. B* **768**, 85 (2007).